**Original Article** | Technology, Experiment, and Physics

eISSN 2005-8330
https://doi.org/10.3348/kjr.2020.0914
Korean J Radiol 2021;22(4):624-633



Korean Journal of Radiology
KJR

# Reliability of Skeletal Muscle Area Measurement on CT with Different Parameters: A Phantom Study

Dong Wook Kim[1*], Jiyeon Ha[1*], Yousun Ko[2], Kyung Won Kim[1], Taeyong Park[3], Jeongjin Lee[4], Myung-Won You[5], Kwon-Ha Yoon[6], Ji Yong Park[1], Young Jin Kee[1], Hong-Kyu Kim[7]

[1]Department of Radiology and Research Institute of Radiology, University of Ulsan College of Medicine, Asan Medical Center, Seoul, Korea; [2]Biomedical Research Center, Asan Institute for Life Sciences, Asan Medical Center, Seoul, Korea; [3]Department of Radiology and Research Institute of Radiology, University of Ulsan College of Medicine, Seoul, Korea; [4]School of Computer Science and Engineering, Soongsil University, Seoul, Korea; [5]Department of Radiology, Kyung Hee University Hospital, Seoul, Korea; [6]Department of Radiology, Wonkwang University College of Medicine, Wonkwang University Hospital, Iksan, Korea; [7]Health Screening & Promotion Center, University of Ulsan College of Medicine, Asan Medical Center, Seoul, Korea

**Objective:** To evaluate the reliability of CT measurements of muscle quantity and quality using variable CT parameters.

**Materials and Methods:** A phantom, simulating the L2–4 vertebral levels, was used for this study. CT images were repeatedly acquired with modulation of tube voltage, tube current, slice thickness, and the image reconstruction algorithm. Reference standard muscle compartments were obtained from the reference maps of the phantom. Cross-sectional area based on the Hounsfield unit (HU) thresholds of muscle and its components, and the mean density of the reference standard muscle compartment, were used to measure the muscle quantity and quality using different CT protocols. Signal-to-noise ratios (SNRs) were calculated in the images acquired with different settings.

**Results:** The skeletal muscle area (threshold, -29 to 150 HU) was constant, regardless of the protocol, occupying at least 91.7% of the reference standard muscle compartment. Conversely, normal attenuation muscle area (30–150 HU) was not constant in the different protocols, varying between 59.7% and 81.7% of the reference standard muscle compartment. The mean density was lower than the target density stated by the manufacturer (45 HU) in all cases (range, 39.0–44.9 HU). The SNR decreased with low tube voltage, low tube current, and in sections with thin slices, whereas it increased when the iterative reconstruction algorithm was used.

**Conclusion:** Measurement of muscle quantity using HU threshold was reliable, regardless of the CT protocol used. Conversely, the measurement of muscle quality using the mean density and narrow HU thresholds were inconsistent and inaccurate across different CT protocols. Therefore, further studies are warranted in future to determine the optimal CT protocols for reliable measurements of muscle quality.

**Keywords:** *Computed tomography; Muscle measurement; Phantom; Sarcopenia*

## INTRODUCTION

Skeletal muscles play a pivotal role in mobile and static functions, including body movement and maintenance of posture [1], and many studies have investigated the relationship of skeletal muscles with physical wellness, morbidity, and mortality [2, 3]. As a result, sarcopenia, defined as the loss of muscle mass and strength, is now formally recognized as a disease with an ICD Code. As the importance of muscle has been emphasized, a variety of

**Received:** July 17, 2020 **Revised:** September 18, 2020 **Accepted:** October 12, 2020
This study was supported by a grant of the Korea Health Technology R&D Project through the Korea Health Industry Development Institute (KHIDI), funded by the Ministry of Health & Welfare, Republic of Korea (grant number: HI18C1216).
*These authors contributed equally to this work.
**Corresponding author:** Kyung Won Kim, MD, PhD, Department of Radiology and Research Institute of Radiology, University of Ulsan College of Medicine, Asan Medical Center, 88 Olympic-ro 43-gil, Songpa-gu, Seoul 05505, Korea.
• E-mail: medimash@gmail.com

Korean Journal of Radiology
KJR

imaging methods have been introduced for the assessment of muscle quantity.

CT is considered as one of the gold-standard methods for noninvasive assessment of muscle quantity [4]. The CT measurement of muscle quantity is based on the difference in the X-ray attenuation value (measured in Hounsfield unit [HU]) of each pixel, as each component of the body (including the skeletal muscles, bone, adipose tissue, and visceral organs) has a specific attenuation threshold [5, 6], which is a prerequisite for their identification in cross-sectional CT images. Thus, additional CT scans, with resulting additional costs and radiation dose, are not needed for muscle evaluation if a CT scan was performed as a part of patient care for any other cause, including the assessment of disease and treatment response.

Recently, the European Working Group on Sarcopenia in Older People 2 revised the definition of sarcopenia by adding muscle function based on muscle quantity to the former definitions; however, muscle quantity by itself is limited in its ability to predict outcomes [7]. Muscle quality, which represents the micro- and macroscopic aspects of muscle architecture and composition, is also related to outcome: intra- and extra-myocellular fat deposition occurs with aging or disuse of muscle and leads to decreased muscle strength and function, followed by increased mortality [8]. As lipid deposition lowers the density of muscles [9], several studies have investigated the measurement of muscle quality using CT—by measuring the muscle density or stratifying the intramuscular components according to their HU distributions—and evaluated its usefulness for determining prognosis, independent of muscle quantity [10-12].

Accordingly, CT has emerged as an accurate measurement tool for the determination of muscle quantity and quality. Nevertheless, standardized parameters for image acquisition [13] have not been determined, and it is questionable whether muscle measurements remain stable if CT parameters are altered. In fact, X-ray attenuation and noise may be influenced by many factors, including tube voltage, tube current, slice thickness, and the reconstruction algorithm used. Variation in these CT parameters might worsen the accuracy of muscle quality measurement if the attenuation threshold is narrowed. Therefore, the aim of our study was to evaluate the reliability of the measurement of muscle quantity and quality under variable CT parameters.

## MATERIALS AND METHODS

This study did not require approval from the Institutional Review Board owing to the study design and because it did not involve any humans/animals.

### Phantom

The CIRS Model 004 CT Simulator (Computerized Imaging Reference Systems, Inc.) was used in this study. This phantom was originally designed to simulate the CT density of the lumbar vertebra, but it also simulates the size, shape, and CT density of the abdominal muscles and subcutaneous adipose tissue at the level of the 2nd to 4th lumbar region. The target CT density of the muscle compartment was 45 HU.

### CT Protocols and Image Acquisitions

CT images of the phantom were acquired on three different systems (Somatom Definition AS+: Siemens Healthineers; Discovery CT750 HD, GE Healthcare; and Ingenuity Core 128, Philips Healthcare). Images were repeatedly obtained at the level of the 3rd lumbar vertebra, with modulation of tube voltage (120 kVp and 80 kVp) and tube current (standard mAs and low mAs), leading to three different categories of radiation dose: standard dose (STD), low dose with reduced voltage (LD-kVp), and low dose with reduced current (LD-mAs). In addition, the slice thickness (thin sections [1 or 1.25 mm], medium sections [2.5 or 3 mm], and thick sections [5 mm]) and image reconstruction algorithms (filtered back projection [FBP] and iterative reconstruction [IR]) were varied. The detailed imaging parameters and their modulations are presented in Table 1.

### Determination of the Reference Standard Muscle Compartment

The reference standard muscle compartment area was determined according to the segmentation of known phantom compartments, including the muscle, subcutaneous fat, visceral fat, internal organs, and vertebra. Each compartment was automatically segmented according to the following processes (Fig. 1).

#### *Preparation: Generation of the Reference Map*

Reference maps of the compartments, including the muscle, subcutaneous fat, visceral fat, internal organs, and vertebra, were generated from known phantom compartments.


https://doi.org/10.3348/kjr.2020.0914

**Table 1. CT Image Acquisition Parameters**

| | Somatom Definition AS+, Siemens Healthineers | Discovery CT750 HD, GE Healthcare | Ingenuity Core 128, Philips Healthcare |
|---|---|---|---|
| Radiation dose* | | | |
| STD | 120 kVp and 220 reference mAs | 120 kVp and 100–400 mA | 120 kVp and 321 reference mAs |
| LD-kVp | 80 kVp and 220 reference mAs | 80 kVp and 100–400 mA | 80 kVp and 321 reference mAs |
| LD-mAs | 120 kVp and 100 reference mAs | 120 kVp and 10–300 mA | 120 kVp and 168 reference mAs |
| Slice thickness* (mm) | | | |
| Thin section | 1 | 1.25 | 1 |
| Medium section | 3 | 2.5 | 3 |
| Thick section | 5 | 5 | 5 |
| Reconstruction algorithm* | FBP<br>IR (SAFIRE, iterative strength level 1) | FBP<br>IR (ASIR 30%) | FBP<br>IR (iDose4) |
| Field of view (mm) | 380 | | |
| Kernel | Standard | | |

*A total of 18 images per device were obtained with the modulation of radiation dose (three conditions), slice thickness (three conditions), and reconstruction algorithm (two conditions). ASIR = adaptive statistical iterative reconstruction, FBP = filtered back projection, IR = iterative reconstruction, LD-kVp = low dose with reduced voltage, LD-mAs = low dose with reduced current, SAFIRE = sinogram affirmed iterative reconstruction, STD = standard dose

#### *Step 1: Initial Segmentation of the Phantom Area*

The area of the phantom on the CT images was separated from the background area using Otsu's thresholding method [14]. Noise reduction using an anisotropic diffusion filter and mathematical morphology was simultaneously performed to generate an initial segmentation of the phantom area [15, 16].

#### *Step 2: Rigid Registration*

The reference map was registered to the initial segmented area (the phantom area) using a center-of-mass match and rigid transformation [17].

#### *Step 3: Final Segmentation of the Muscle Compartment*

The muscle compartment was segmented using the reference map.

### Measurement of Muscle Area and Density

For the CT images acquired with different parameters, the cross-sectional areas of the muscle and its components were segmented using pre-defined HU thresholds that were deemed generally acceptable in previous studies (Fig. 2) [11]. The total muscle area was segmented using a threshold of -190 to 150 HU. The total muscle area component was categorized into skeletal muscle areas (SMA) with a threshold of -29 to 150 HU, and intermuscular adipose tissue areas (IMA) with a threshold of -190 to -30 HU. The SMA was further subcategorized into normal attenuation muscle area (NAMA; threshold, 30 to 150 HU) and low attenuation muscle area (LAMA; threshold, -29 to 29 HU) to facilitate evaluation of the quality of muscle according to CT density [11, 18]. The mean density of the reference standard muscle compartment was calculated by averaging the HU value of each pixel within the area. A web-based toolkit for automatic measurement of muscle area is available at https://iaidimage.com/app/aid-u/sarcopenia-l3.

### Signal-to-Noise Ratio Analysis

The signal-to-noise ratio (SNR) was analyzed using the ImageJ program (National Institute of Health, https://imagej.nih.gov/ij). In the phantom CT images, the regions of interest were placed in the right paraspinal muscle and the air outside the phantom. The standard deviation of the air outside the phantom was regarded as background image noise, and the SNR was calculated by dividing the mean attenuation of the right paraspinal muscle by the background image noise [19].

### Statistical Analysis

The mean values obtained from the three devices using the same parameters were used as representative values. The results obtained using different parameters were compared with those obtained with the standard protocol (i.e., STD with FBP reconstruction and thick sections [5 mm]) and with the pre-segmented area. In addition, the Dice similarity coefficient (DSC) [20] was used to evaluate the similarities of the cross-sectional areas of the total


https://doi.org/10.3348/kjr.2020.0914

Korean Journal of Radiology
KJR

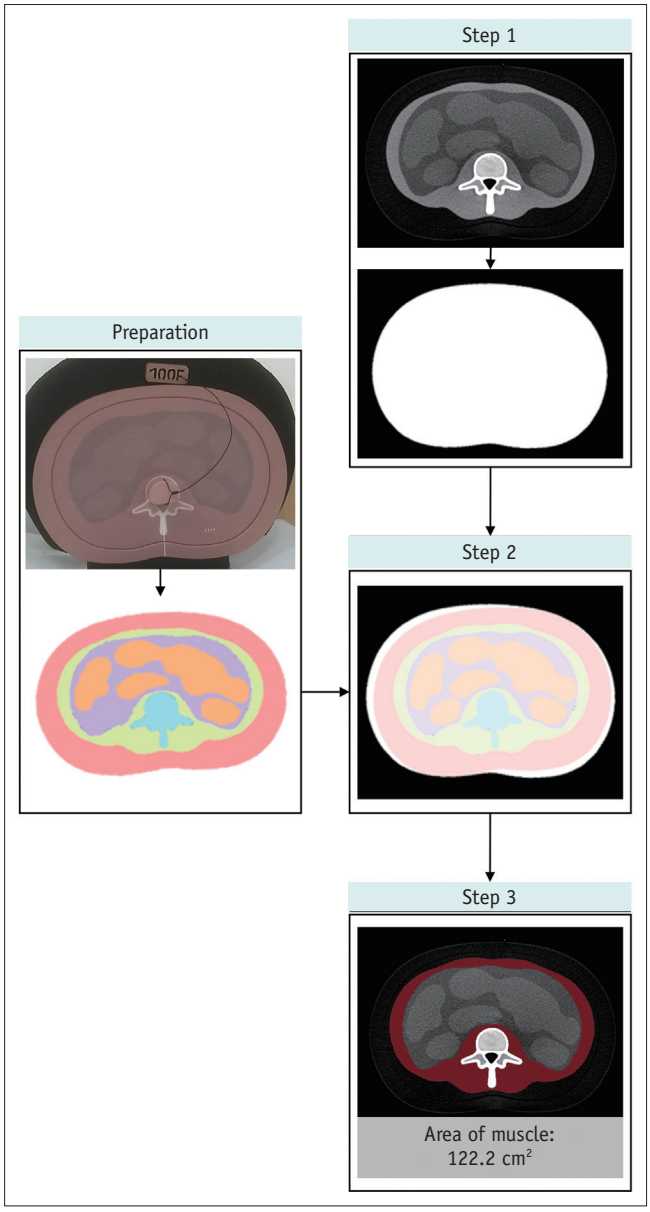


**Fig. 1. Determination of the reference standard muscle compartment.** The reference standard muscle compartment was determined using the following process: separation of the phantom area from the background area on the CT image (step 1), rigid registration of the reference map (preparation) onto the phantom area (step 2), and segmentation of the muscle compartment (step 3). The final area of muscle on the CT image was 122.2 $cm^2$.

muscle area, SMA, and NAMA with the use of CT parameters different from those in the standard protocol.

The Wilcoxon signed-rank test was used to evaluate the relationships of the SNR and background noise to tube voltage, radiation dose, and reconstruction algorithm. The Friedman test was used to evaluate the SNR and background noise with different slice thicknesses. Statistical analysis was performed with PASW 18 (SPSS Inc.), and a $p$ value < 0.05 was considered statistically significant.

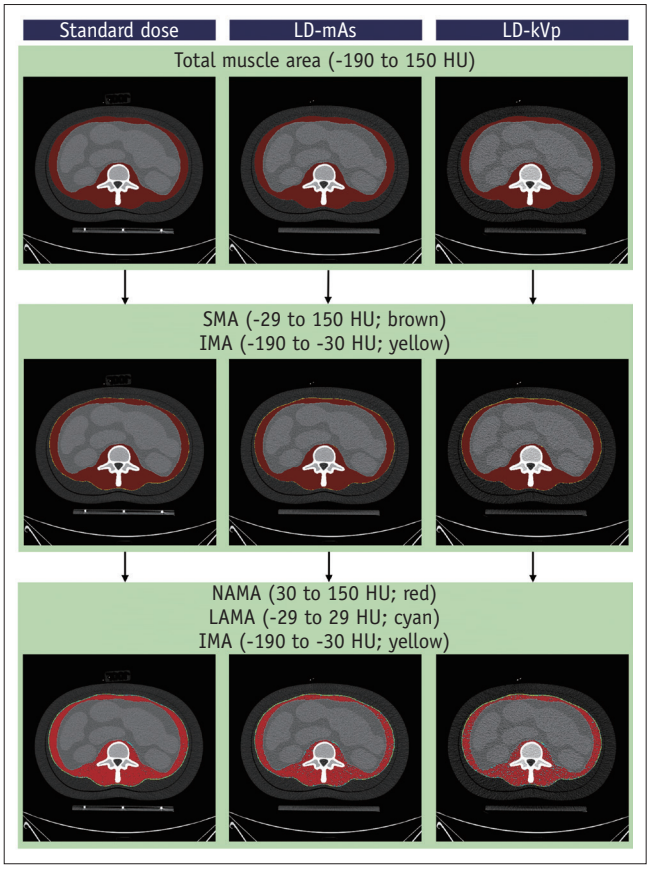


**Fig. 2. Segmentation of the muscle compartment and its components using HU thresholds.** The components are the areas segmented using HU thresholds to represent biological and clinical tissue components, including SMA (composed of NAMA and LAMA) and IMA. HU = Hounsfield unit, IMA = intermuscular adipose tissue area, LAMA = low attenuation muscle area, LD-kVp = low dose with reduced voltage, LD-mAs = low dose with reduced current, NAMA = normal attenuation muscle area, SMA = skeletal muscle area

## RESULTS

A total of 18 image sets were acquired, including various combinations of imaging parameters, three radiation dose settings (STD, LD-mAs, and LD-kVp protocols), three different slice thicknesses (thin, medium, and thick sections), and two different reconstruction algorithms (FBP and IR).

### Impact of CT Parameters on Segmentation Area

Compared with the reference standard muscle compartment, the segmented SMA values were higher with both the STD and the LD-mAs protocols, while they were lowest with the LD-kVp protocol, regardless of the slice thickness and reconstruction algorithm (Fig. 3). The


https://doi.org/10.3348/kjr.2020.0914

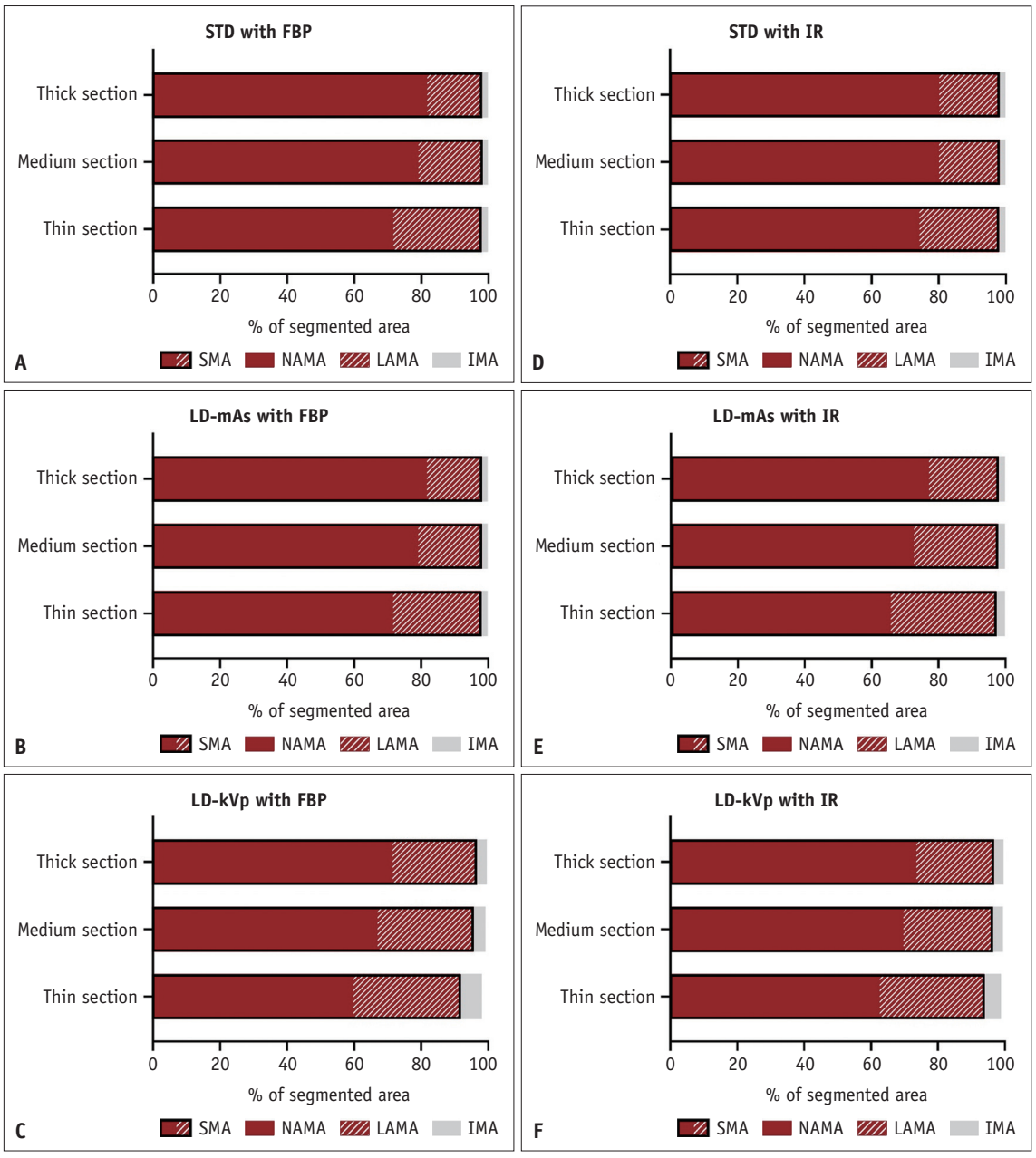


**Fig. 3. Proportions of the segmented areas of muscle components with different CT protocols (A-F).** The area including NAMA and LAMA represents SMA. FBP = filtered back projection, IMA = intermuscular adipose tissue area, IR = iterative reconstruction, LAMA = low attenuation muscle area, LD-kVp = low dose with reduced voltage, LD-mAs = low dose with reduced current, NAMA = normal attenuation muscle area, SMA = skeletal muscle area, STD = standard dose

SMA results did not differ significantly between the thin, medium, and thick sections, or between the different reconstruction algorithms.

In all the CT protocols, SMA occupied at least 91.7% of the pre-segmented area. In contrast, NAMA was not constant across the protocols, varying between 59.7% and 81.7% of the pre-segmented area, despite the fact that the target HU of the muscle stated by the manufacturer (45 HU) was within the threshold range. Of note, the proportions of SMA and NAMA in the images generated using IR algorithm were higher than those in the images generated using FBP algorithm in all but the standard protocol, although the differences for SMA and NAMA were less than 2.7% and 4.7%, respectively.

The muscle area and SMA both showed good similarity, with the DSCs being within the range of 0.96–1.00 for the muscle area and 0.94–1.00 for the SMA. However, the DSCs of NAMA ranged from 0.74 to 0.96, showing variation that


https://doi.org/10.3348/kjr.2020.0914

Korean Journal of Radiology
KJR

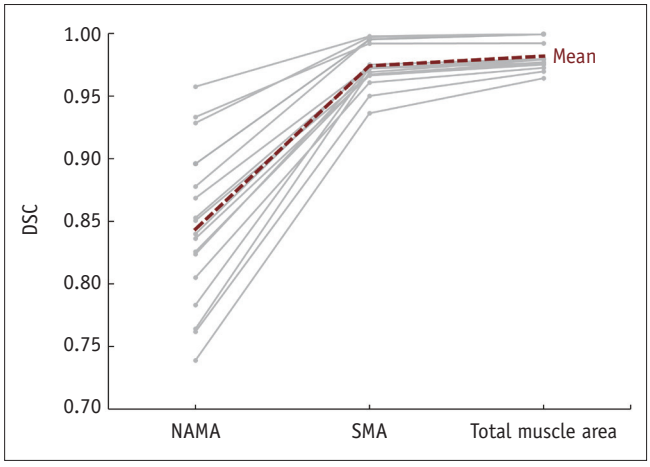


**Fig. 4. DSC between the variable protocols and standard protocol.** DSC = Dice similarity coefficient, NAMA = normal attenuation muscle area, SMA = skeletal muscle area

was dependent on the CT parameters (Fig. 4).

### Impact of CT Parameters on Density

In all cases, the mean density of the reference standard muscle compartment was lower than the target density stated by the manufacturer (range, 39.0–44.9 HU) (Fig. 5). The mean density increased with thin slices (difference range, 0–1.3 HU) and low tube voltage (difference range, 3.4–3.5 HU), but decreased with low radiation dose (difference range, 1.01.8 HU) and IR usage (difference range, -0.1–1.2 HU).

### Signal-to-Noise Ratio

The background noise increased with low tube voltage (120 kVp vs. 80 kVp: 6.55 vs. 12.75; $p < 0.001$) and low tube current (standard vs. low: 6.55 vs. 8.85; $p < 0.001$) (Table 2). In association with the changes in background noise, the SNR decreased with low tube voltage (120 kVp vs. 80 kVp: 5.92 vs. 3.21; $p < 0.001$) and low tube current (standard vs. low: 5.92 vs. 4.78; $p < 0.001$). Background noise decreased with thicker sections (1 [or 1.25] vs. 3 [or 2.5] vs. 5: 12.60 vs. 8.80 vs. 7.35; $p < 0.001$), while SNR increased with thicker sections (1 [or 1.25] vs. 3 [or 2.5] vs. 5: 3.41 vs. 5.04 vs. 5.53; $p < 0.001$). Images reconstructed with IR algorithm showed lower background noise (IR vs. FBP: 9.20 vs. 10.90; $p = 0.002$) and higher SNR (IR vs. FBP: 4.83 vs. 3.78; $p = 0.005$) than those reconstructed with FBP algorithm.

## DISCUSSION

To the best of our knowledge, no consensus exists over which CT protocols or parameters yield the most reliable muscle measurements. Although many studies have investigated the assessment of muscle quantity and quality, they have not provided the CT acquisition parameters in sufficient detail [21], which has hampered the reproduction of their work. In this phantom study, we investigated the reliability of CT measurement of muscle quantity and quality with different CT parameters, using two popular methods for measuring muscle quantity and quality on CT: using 1) the cross-sectional area within the defined HU thresholds, and 2) the mean density. In addition, we used the DSC to evaluate similarities in cross-sectional area over different acquisitions using different parameters, relative to the standard protocol acquisitions. According to our findings, the cross-sectional total muscle areas (-190 to 150 HU) and SMA (-29 to 150 HU) with different protocols were similar to those using the standard protocol, whereas the areas of NAMA (30 to 150 HU) were not stable across the protocols. Furthermore, the mean density of the muscle compartment was inaccurate and fell short of the target attenuation stated by the manufacturer.

The most popular attenuation threshold used to measure muscle mass (or quantity) is -29 to 150 HU. In addition, the lower margin might be expanded to -190 HU to consider the IMA component. Our study revealed that the measurement of muscle quantity using these thresholds was reliable irrespective of the CT parameters used, consistent with the report of a prior study involving human subjects which reported that SMA measured with thin slice thickness and low radiation dose was constant (lower by less than 5%) [22]. In contrast, the measurement of muscle quality using the mean density of the muscle compartment should be interpreted with caution. It is evident that fat deposition in muscle, which is related to poor muscle strength, mortality, and morbidity, lowers the mean CT density [8, 9]. However, our study revealed that the mean CT density was subject to the choice of CT parameters. Fuchs et al. [22] also reported that thin slices (2 mm vs. 5 mm thickness) and low radiation dose altered the mean density by 4.8 and 17.3 HU, respectively. In principle, the mean HU values should be constant irrespective of the radiation dose used, as the outliers of HU, caused by noise, at both ends of the range should offset each other [22]. However, this was not the case for the reference standard muscle compartment used in our study, probably because noise from neighboring structures, such as the vertebrae and adipose tissue, altered the attenuation of the affected pixels. Moreover,


https://doi.org/10.3348/kjr.2020.0914

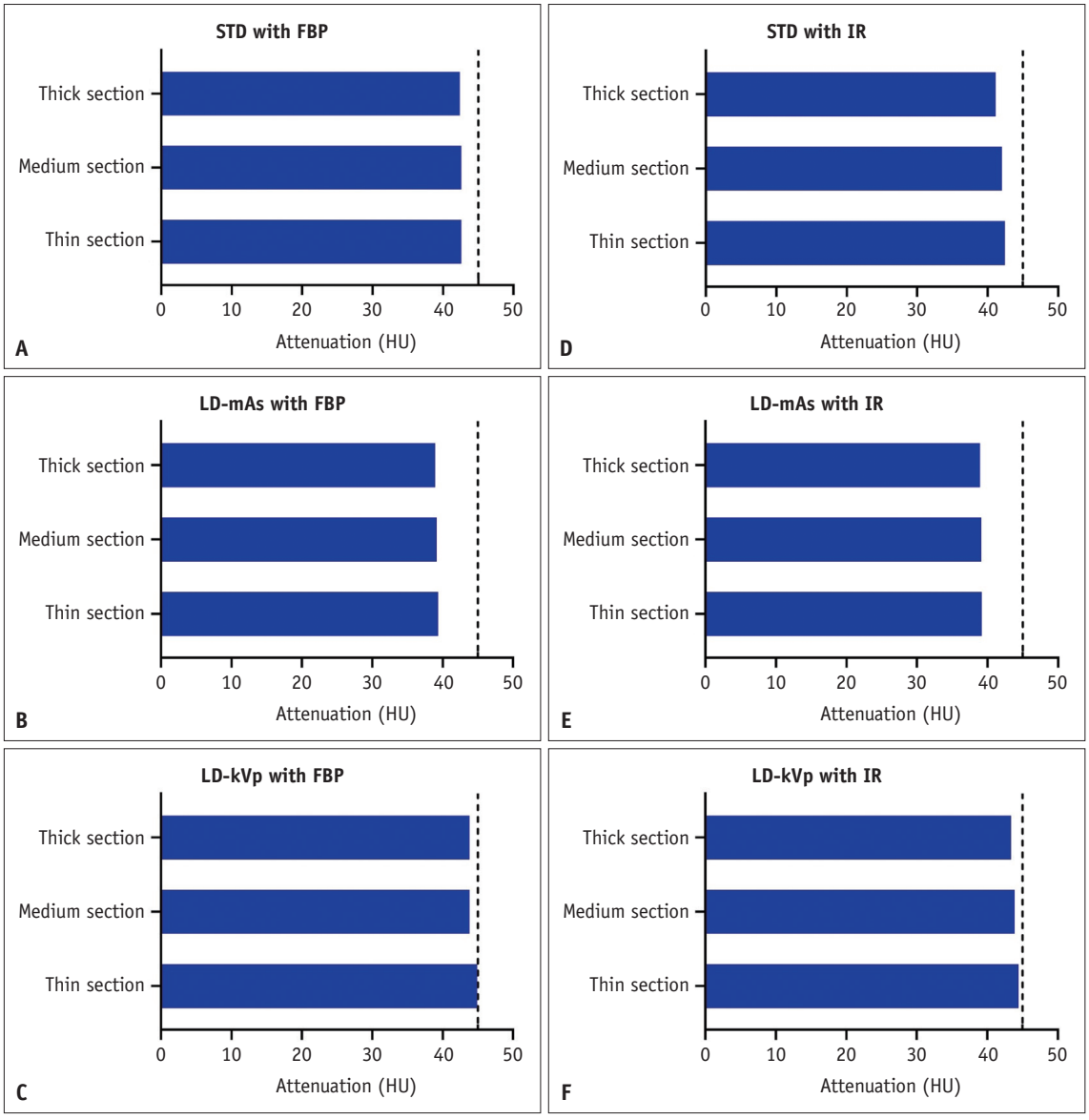


**Fig. 5. Mean density of the muscle compartment with different protocols (A-F).** Dashed lines indicate the target density of skeletal muscle (45 HU). FBP = filtered back projection, HU = Hounsfield unit, IR = iterative reconstruction, LD-kVp = low dose with reduced voltage, LD-mAs = low dose with reduced current, STD = standard dose

in CT images with low SNR, such as those acquired with protocols using low tube current, low tube voltage, or thin slice sections, the effect could become substantial. The photoelectric effect along with the low tube voltage might have altered the CT density [23, 24].

Some studies have suggested differentiating low attenuation muscle from normal attenuation muscle on the basis of the HU threshold (usually using a cutoff of 30 HU) [11, 25]. However, according to our results, the measurement of muscle quality based on this narrower HU threshold would not be constant across different protocols. The reliability of muscle quality evaluation across protocols would most likely be worse if differentiation based on this threshold was applied to human subjects, as intra- and extra-cellular fat components actually exist within the muscle tissue of real subjects, unlike in our phantom [26]. Therefore, we suggest that the CT measurement of muscle quality should use only a limited range of CT parameter settings. However, further studies are required in future to determine which parameters should be adopted for reliable measurements.

We also investigated the usefulness of the IR algorithm for muscle measurement on dose-reduced protocols; we expected the reduced noise to better reflect the true


https://doi.org/10.3348/kjr.2020.0914

Korean Journal of Radiology
KJR

**Table 2. Background Image Noise and SNRs of Phantom Images with Different Protocols**

| Protocol | Background Noise | | | SNR* | | |
|---|---|---|---|---|---|---|
| | Median | IQR | *P** | Median | IQR | *P** |
| Tube voltage (kVp) | | | < 0.001 | | | < 0.001 |
| 120 (n = 18) | 6.55 | 6.05, 9.95 | | 5.92 | 4.24, 7.77 | |
| 80 (n = 18) | 12.75 | 10.70, 19.00 | | 3.21 | 2.48, 3.82 | |
| Tube current (mAs) | | | < 0.001 | | | < 0.001 |
| Standard (n = 18) | 6.55 | 6.05, 9.95 | | 5.92 | 4.24, 7.77 | |
| Low (n = 18) | 8.85 | 7.63, 11.53 | | 4.78 | 3.61, 5.57 | |
| Slice thickness (mm) | | | < 0.001 | | | < 0.001 |
| 1 or 1.25 (n = 18) | 12.60 | 11.20, 19.68 | | 3.41 | 2.66, 3.83 | |
| 2.5 or 3 (n = 18) | 8.80 | 7.35, 11.33 | | 5.04 | 3.60, 5.82 | |
| 5 (n = 18) | 7.35 | 6.28, 9.90 | | 5.53 | 4.21, 7.12 | |
| Reconstruction algorithm | | | 0.002 | | | 0.005 |
| FBP (n = 27) | 10.90 | 7.30, 13.80 | | 3.78 | 3.30, 5.66 | |
| IR (n = 27) | 9.20 | 7.40, 11.60 | | 4.83 | 3.51, 5.79 | |

*Using the Wilcoxon signed-rank test (tube voltage, radiation dose, and reconstruction algorithm) or Friedman test (slice thickness). FBP = filtered back projection, IQR = interquartile range, IR = iterative reconstruction, SNR = signal-to-noise ratio

attenuation value of each pixel. In fact, the SMA and NAMA in the images generated using the IR algorithm occupied more pre-segmented areas than they did in images acquired with the same protocols but reconstructed using the FBP algorithm. Images acquired using the standard protocol, which implied sufficient image quality for the measurement, were the only exceptions to this tendency. Nevertheless, the difference between the IR and FBP algorithms was trivial in all cases, such that the improvement in noise was insufficient for muscle quality assessment using the narrow HU threshold (e.g., 29–150 HU) to be reliable with the low-dose protocols. In addition, the mean HU increased with the IR algorithm, except in the case of low tube voltage with a 3-mm thickness. However, consistent with the results of prior studies [27-29], the difference was small, less than 1.2 HU.

Our study has several limitations. First, the phantom did not fully reflect the muscle components of the human body, as the HU of the muscle area was theoretically constant in the phantom. Moreover, as the phantom was primarily used to measure bone density, measurement of muscle density might have been inaccurate. Thus, the measured mean HU values of the muscle compartment were all lower than the true value (i.e., 45 HU), irrespective of the CT parameters. Nevertheless, using the phantom, we could investigate the reliability of measurements in relation to CT parameters, as we could adjust the CT parameters without any ethical considerations of radiation dose. However, additional animal or clinical studies might be required in future to confirm our results. Second, contrast agent administration would also influence the reliability of muscle measurement, and it was not possible to assess this using a phantom. In fact, many studies have reported that contrast usage and its enhancement phase alters the interpretation of muscle quantity and quality [22, 30, 31]. Lastly, we did not investigate the reliability of muscle measurement across different scanners. However, we believe that it was impractical to compare them head-to-head, as each device has innate strengths and limitations in terms of dose reduction and image reconstruction. In addition, the aim of this study was not to determine which device was superior; rather, we wanted to determine the constant effects of alterations to the protocols, irrespective of the device characteristics.

In conclusion, the measurement of muscle quantity using HU threshold is a reliable method, regardless of the CT protocol used. Conversely, the measurement of muscle quality using the mean CT density and a narrower HU threshold was inconsistent and inaccurate, with variations across the different CT protocols. Therefore, future studies are warranted to determine the optimal CT protocols for reliable measurements of muscle quality.

## Conflicts of Interest

The authors have no potential conflicts of interest to disclose.

## Author Contributions

Conceptualization: Kyung Won Kim. Data curation: Dong Wook Kim, Jiyeon Ha, Yousun Ko. Formal analysis: Dong

 https://doi.org/10.3348/kjr.2020.0914 

Wook Kim, Taeyong Park. Funding acquisition: Kyung Won Kim. Investigation: Jiyeon Ha, Myung-Won You, Kwon-Ha Yoon. Methodology: Dong Wook Kim, Kyung Won Kim. Project administration: Yousun Ko, Kyung Won Kim, Jeongjin Lee. Resources: Kyung Won Kim, Myung-Won You, Kwon-Ha Yoon. Software: Taeyong Park, Jeongjin Lee, Ji Yong Park, Young Jin Kee. Supervision: Hong-Kyu Kim. Visualization: Yousun Ko, Taeyong Park. Writing—original draft: Dong Wook Kim, Jiyeon Ha, Taeyong Park. Writing—review & editing: Yousun Ko, Kyung Won Kim, Jeongjin Lee, Myung-Won You, Hong-Kyu Kim.

### ORCID iDs

Dong Wook Kim
https://orcid.org/0000-0001-7887-657X
Jiyeon Ha
https://orcid.org/0000-0003-3496-4134
Yousun Ko
https://orcid.org/0000-0002-2181-9555
Kyung Won Kim
https://orcid.org/0000-0002-1532-5970
Taeyong Park
https://orcid.org/0000-0002-7523-8975
Jeongjin Lee
https://orcid.org/0000-0001-9676-271X
Myung-Won You
https://orcid.org/0000-0001-6262-5784
Kwon-Ha Yoon
https://orcid.org/0000-0002-2634-8510
Ji Yong Park
https://orcid.org/0000-0003-4059-1979
Young Jin Kee
https://orcid.org/0000-0003-0929-284X
Hong-Kyu Kim
https://orcid.org/0000-0002-7606-3521

## REFERENCES

1. Frontera WR, Ochala J. Skeletal muscle: a brief review of structure and function. *Calcif Tissue Int* 2015;96:183-195
2. Prado CM, Lieffers JR, McCargar LJ, Reiman T, Sawyer MB, Martin L, et al. Prevalence and clinical implications of sarcopenic obesity in patients with solid tumours of the respiratory and gastrointestinal tracts: a population-based study. *Lancet Oncol* 2008;9:629-635
3. Martin L, Birdsell L, Macdonald N, Reiman T, Clandinin MT, McCargar LJ, et al. Cancer cachexia in the age of obesity: skeletal muscle depletion is a powerful prognostic factor, independent of body mass index. *J Clin Oncol* 2013;31:1539-1547
4. Beaudart C, McCloskey E, Bruyère O, Cesari M, Rolland Y, Rizzoli R, et al. Sarcopenia in daily practice: assessment and management. *BMC Geriatr* 2016;16:170
5. Prado CM, Heymsfield SB. Lean tissue imaging: a new era for nutritional assessment and intervention. *JPEN J Parenter Enteral Nutr* 2014;38:940-953
6. Tosato M, Marzetti E, Cesari M, Savera G, Miller RR, Bernabei R, et al. Measurement of muscle mass in sarcopenia: from imaging to biochemical markers. *Aging Clin Exp Res* 2017;29:19-27
7. Cruz-Jentoft AJ, Bahat G, Bauer J, Boirie Y, Bruyère O, Cederholm T, et al. Sarcopenia: revised European consensus on definition and diagnosis. *Age Ageing* 2019;48:16-31
8. Reinders I, Murphy RA, Brouwer IA, Visser M, Launer L, Siggeirsdottir K, et al. Muscle quality and myosteatosis: novel associations with mortality risk: the Age, Gene/Environment Susceptibility (AGES)-Reykjavik Study. *Am J Epidemiol* 2016;183:53-60
9. Goodpaster BH, Kelley DE, Thaete FL, He J, Ross R. Skeletal muscle attenuation determined by computed tomography is associated with skeletal muscle lipid content. *J Appl Physiol (1985)* 2000;89:104-110
10. Lang T, Cauley JA, Tylavsky F, Bauer D, Cummings S, Harris TB; Health ABC Study. Computed tomographic measurements of thigh muscle cross-sectional area and attenuation coefficient predict hip fracture: the health, aging, and body composition study. *J Bone Miner Res* 2010;25:513-519
11. Aubrey J, Esfandiari N, Baracos VE, Buteau FA, Frenette J, Putman CT, et al. Measurement of skeletal muscle radiation attenuation and basis of its biological variation. *Acta Physiol (Oxf)* 2014;210:489-497
12. Goodpaster BH, Thaete FL, Simoneau JA, Kelley DE. Subcutaneous abdominal fat and thigh muscle composition predict insulin sensitivity independently of visceral fat. *Diabetes* 1997;46:1579-1585
13. Buckinx F, Landi F, Cesari M, Fielding RA, Visser M, Engelke K, et al. Pitfalls in the measurement of muscle mass: a need for a reference standard. *J Cachexia Sarcopenia Muscle* 2018;9:269-278
14. Otsu N. A threshold selection method from gray-level histograms. *IEEE T Syst Man Cy-S* 1979;9:62-66
15. Weickert J. *Anisotropic diffusion in image processing*. Stuttgart: Teubner, 1998
16. Haralick RM, Sternberg SR, Zhuang X. Image analysis using mathematical morphology. *IEEE Trans Pattern Anal Mach Intell* 1987;9:532-550
17. Hill DL, Batchelor PG, Holden M, Hawkes DJ. Medical image registration. *Phys Med Biol* 2001;46:R1-45
18. Goodpaster BH, Kelley DE, Wing RR, Meier A, Thaete FL. Effects of weight loss on regional fat distribution and insulin sensitivity in obesity. *Diabetes* 1999;48:839-847
19. Duan X, Wang J, Leng S, Schmidt B, Allmendinger T, Grant K,


https://doi.org/10.3348/kjr.2020.0914

et al. Electronic noise in CT detectors: impact on image noise and artifacts. *AJR Am J Roentgenol* 2013;201:W626-W632
20. Dice LR. Measures of the amount of ecologic association between species. *Ecology* 1945;26:297-302
21. Amini B, Boyle SP, Boutin RD, Lenchik L. Approaches to assessment of muscle mass and myosteatosis on computed tomography: a systematic review. *J Gerontol A Biol Sci Med Sci* 2019;74:1671-1678
22. Fuchs G, Chretien YR, Mario J, Do S, Eikermann M, Liu B, et al. Quantifying the effect of slice thickness, intravenous contrast and tube current on muscle segmentation: implications for body composition analysis. *Eur Radiol* 2018;28:2455-2463
23. van der Werf A, Dekker IM, Meijerink MR, Wierdsma NJ, de van der Schueren MAE, Langius JAE. Skeletal muscle analyses: agreement between non-contrast and contrast CT scan measurements of skeletal muscle area and mean muscle attenuation. *Clin Physiol Funct Imaging* 2018;38:366-372
24. Nakayama Y, Awai K, Funama Y, Hatemura M, Imuta M, Nakaura T, et al. Abdominal CT with low tube voltage: preliminary observations about radiation dose, contrast enhancement, image quality, and noise. *Radiology* 2005;237:945-951
25. Lee S, Kuk JL, Davidson LE, Hudson R, Kilpatrick K, Graham TE, et al. Exercise without weight loss is an effective strategy for obesity reduction in obese individuals with and without Type 2 diabetes. *J Appl Physiol (1985)* 2005;99:1220-1225
26. Rogalla P, Meiri N, Hoksch B, Boeing H, Hamm B. Low-dose spiral computed tomography for measuring abdominal fat volume and distribution in a clinical setting. *Eur J Clin Nutr* 1998;52:597-602
27. Singh S, Kalra MK, Do S, Thibault JB, Pien H, O'Connor OJ, et al. Comparison of hybrid and pure iterative reconstruction techniques with conventional filtered back projection: dose reduction potential in the abdomen. *J Comput Assist Tomogr* 2012;36:347-353
28. Singh S, Kalra MK, Hsieh J, Licato PE, Do S, Pien HH, et al. Abdominal CT: comparison of adaptive statistical iterative and filtered back projection reconstruction techniques. *Radiology* 2010;257:373-383
29. Singh S, Kalra MK, Gilman MD, Hsieh J, Pien HH, Digumarthy SR, et al. Adaptive statistical iterative reconstruction technique for radiation dose reduction in chest CT: a pilot study. *Radiology* 2011;259:565-573
30. Paris MT, Furberg HF, Petruzella S, Akin O, Hötker AM, Mourtzakis M. Influence of contrast administration on computed tomography–based analysis of visceral adipose and skeletal muscle tissue in clear cell renal cell carcinoma. *JPEN J Parenter Enteral Nutr* 2018;42:1148-1155
31. van Vugt JLA, Coebergh van den Braak RRJ, Schippers HJW, Veen KM, Levolger S, de Bruin RWF, et al. Contrast-enhancement influences skeletal muscle density, but not skeletal muscle mass, measurements on computed tomography. *Clin Nutr* 2018;37:1707-1714